0026-895X/04/6601-45–55$20.00
MOLECULAR PHARMACOLOGY
Copyright © 2004 The American Society for Pharmacology and Experimental Therapeutics
Mol Pharmacol 66:45–55, 2004

Vol. 66, No. 1
3225/1156958
Printed in U.S.A.

The Exchanger Inhibitory Peptide Region-Dependent Inhibition of Na^+/Ca^{2+} Exchange by SN-6 [2-[4-(4-Nitrobenzyloxy)benzyl]thiazolidine-4-carboxylic Acid Ethyl Ester], a Novel Benzyloxyphenyl Derivative

Takahiro Iwamoto, Yutaka Inoue, Kazuhiko Ito, Takahiro Sakaue, Satomi Kita, and Takeshi Katsuragi

Department of Pharmacology, School of Medicine, Fukuoka University, Fukuoka, Japan (T.I., S.K., T.K.); Molecular Physiology, National Cardiovascular Center Research Institute, Osaka, Japan (T.I.); Research Laboratory, Senju Pharmaceutical Co. Ltd., Kobe, Japan (Y.I., K.I.); and Global Pharmacovigilance Post Marketing Surveillance Department, Senju Pharmaceutical Co. Ltd., Osaka, Japan (T.S.)

Received January 21, 2004; accepted March 18, 2004

This article is available online at http://molpharm.aspetjournals.org

ABSTRACT

We investigated the properties and interaction domains of SN-6 [2-[4-(4-nitrobenzyloxy)benzyl]thiazolidine-4-carboxylic acid ethyl ester], a newly synthesized and selective Na^+/Ca^{2+} exchange (NCX) inhibitor. SN-6 (0.3–30 μM) inhibited preferentially intracellular Na^+-dependent $^{45}Ca^{2+}$ uptake (i.e., the reverse mode) compared with extracellular Na^+-dependent $^{45}Ca^{2+}$ efflux (i.e., the forward mode) in NCX1-transfected fibroblasts. SN-6 was 3- to 5-fold more inhibitory to $^{45}Ca^{2+}$ uptake in NCX1 (IC_{50} = 2.9 μM) than to that in NCX2 or NCX3 but not to that in NCKX2. We searched for regions that may form the SN-6 receptor by NCX1/NCX3-chimeric analyses and determined that amino acid regions 73 to 108 and 193 to 230 in NCX1 are mostly responsible for the differential drug response between NCX1 and NCX3. Further site-directed mutagenesis revealed that double substitutions of Val227 and Tyr228 in NCX1, which exist within the exchanger inhibitory peptide (XIP) region, mimicked the different drug response. In addition, F213R, G833C, and N839A mutations in NCX1 resulted in loss of drug sensitivity. Exchangers with mutated XIP regions, which display either undetectable or accelerated Na^+-dependent inactivation, had markedly reduced sensitivity or hypersensitivity to SN-6, respectively. Cell ATP depletion enhanced the inhibitory potency of SN-6. Therefore, SN-6 at lower doses (IC_{50} = 0.63 μM) potently protected against hypoxia/reoxygenation-induced cell damage in renal tubular cells overexpressing NCX1, suggesting that this drug predominantly works under hypoxic/ischemic conditions. These properties of SN-6, which may be derived from its interaction with the XIP region, are advantageous to developing it as a new anti-ischemic drug.

The Na^+/Ca^{2+} exchanger (NCX) is a bidirectional transporter that is controlled by membrane potential and transmembrane gradients of Na^+ and Ca^{2+} (Blaustein and Lederer, 1999; Philipson and Nicoll, 2000; Shigekawa and Iwamoto, 2001). In cardiac muscle, the exchanger plays the primary role in the extrusion of intracellular Ca^{2+} (Ca^{2+}_i) during each excitation-contraction coupling (Bers, 2002). Under pathological conditions such as cardiac ischemia/reperfusion injury, the exchanger is believed to cause Ca^{2+} overload attributable to elevated intracellular Na^+ (Na^+_i) concentration (Tani, 1990), leading to mechanical and electrical dysfunction of cardiomyocytes.

Mammalian NCX forms a multigene family comprising NCX1, NCX2, and NCX3. NCX1 is highly expressed in the heart, kidney, and brain and at much lower levels in other tissues, whereas the expression of NCX2 and NCX3 is limited mainly to the brain and skeletal muscle (Quednau et al., 1997). These three isoforms presumably have similar molecular topologies consisting of nine transmembrane segments and a large central cytoplasmic loop (Iwamoto et al., 1999a; Nicoll et al., 1999). The former part, particularly the α-repeat regions, may participate in ion transport (Nicoll et al., 1996; Doering et al., 1998; Iwamoto et al., 2000); the latter part, possessing the exchanger inhibitory

This work was supported by a Grant-in-Aid 14570097 for scientific research (to T.I.) from the Ministry of Education, Science and Culture of Japan and grant No.02 from the Salt Science Research Foundation (to T.I.).

ABBREVIATIONS: NCX, Na^+/Ca^{2+} exchanger; SN-6, 2-[4-(4-nitrobenzyloxy)benzyl]thiazolidine-4-carboxylic acid ethyl ester; KB-R7943, 2-[2-[4-(4-nitrobenzyloxyl)phenyl]ethyl]isothiourea methanesulfonate; SEA0400, 2-[4-[(2,5-difluorophenyl)methoxy]phenoxy]-5-ethoxyaniline; XIP, exchanger inhibitory peptide; DMEM, Dulbecco's modified Eagle's medium; FCS, fetal calf serum; BSS, balanced salt solution; QNB, L-quinuclidinyl benzilate; LDH, lactate dehydrogenase; MOPS, 3-(*N*-morpholino)propanesulfonic acid.

peptide (XIP) region (Li et al., 1991; Matsuoka et al., 1997) and regulatory Ca^{2+} binding sites (Levitsky et al., 1994; Matsuoka et al., 1995), is primarily involved in various regulatory properties. NCX1 has been shown to be secondarily regulated by the transport substrates Na^+ and Ca^{2+} (Hilgemann et al., 1992a,b). $Ca^{2+}{}_i$ at the submicromolar level activates NCX activity by promoting the recovery of the exchanger from the "I_2 inactivation state", whereas high $Na^+{}_i$ restrains the exchange by facilitating the entry of the exchanger into the "I_1 inactivation state".

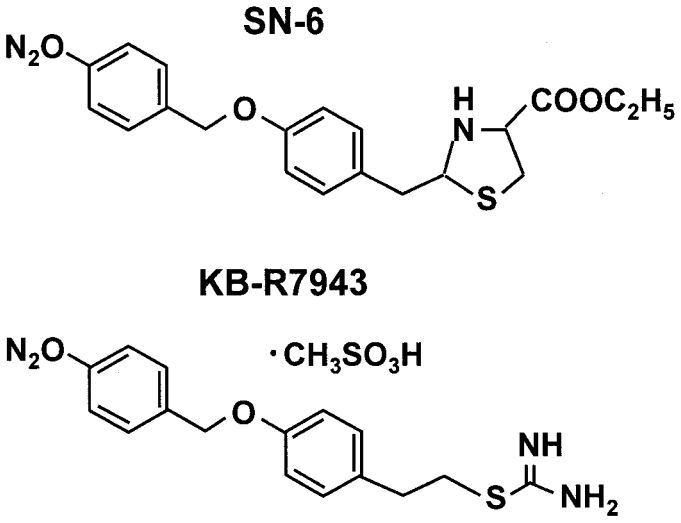

Fig. 1. Chemical structures of benzyloxyphenyl derivatives SN-6 and KB-R7943.

A selective NCX inhibitor will be very useful in the study of NCX's physiological and pathophysiological roles and to clarify the reaction mechanism of this transporter. Moreover, such an inhibitor may have therapeutic potential as a new remedy for several ischemic diseases, arrhythmias, heart failure, and essential hypertension. KB-R7943, a benzyloxyphenyl derivative, was first introduced in 1996 as a selective NCX inhibitor (Iwamoto et al., 1996; Watano et al., 1996). In 2001, Matsuda et al. reported on SEA0400, a newly developed, potent, and selective inhibitor of NCX. The inhibitory potency of SEA0400 is 80 to 100 times more powerful than that of KB-R7943. SEA0400 has an excellent specificity; KB-R7943 possesses nonspecific actions against ion channels, neuronal nicotinic acetylcholine receptors, the *N*-methyl-D-aspartate receptor, and the norepinephrine transporter (Watano et al., 1996; Sobolevsky and Khodorov, 1999; Pintado et al., 2000; Matsuda et al., 2001). However, Reuter et al. (2002) suggested recently that SEA0400, too, has unknown nonspecific effects.

These NCX inhibitors have several interesting features: KB-R7943 and SEA0400 inhibit the reverse mode (i.e., Ca^{2+}

TABLE 1
Effects of SN-6 on receptors and ion channels
Binding assays with several ligands were performed using native or recombinant receptors. Data shown are means ± S.E. of three independent experiments.

	Ligand	Source	IC_{50}
			μM
Receptors			
Adenosine			
A_1	[^{3}H]DPCPX	Human recombinant	>30
A_{2A}	[^{3}H]CGS-21680	Human recombinant	>30
A_{2B}	[^{3}H]DPCPX	Human recombinant	>30
A_3	^{125}I-AB-MECA	Rat recombinant	>30
Adrenergic			
α_1	[^{3}H]Prazosin	Rat brain	>30
α_2	[^{3}H]Rauwolscine	Rat cerebral cortex	>30
β_1	^{125}I-Cyanopindolol	Human recombinant	>30
β_2	[^{3}H]CGP-12177	Human recombinant	>30
β_3	^{125}I-Cyanopindolol	Human recombinant	>30
Cholinergic			
mACh	[^{3}H]QNB	Rat cerebral cortex	18 ± 1.5
Glutamate			
AMPA	[^{3}H]AMPA	Rat cerebral cortex	>30
Kainate	[^{3}H]Kainate	Rat brain	>30
NMDA	[^{3}H]CGP-39653	Rat cerebral cortex	>30
Bradykinin			
B_1	[^{3}H]Des-Arg^{10}-Kallidin	Human recombinant	>30
B_2	[^{3}H]Bradykinin	Human recombinant	>30
Ion channels			
L-type Ca^{2+} channel			
Benzothiazepine	[^{3}H]Diltiazem	Rat brain	>30
Diphydropyridine	[^{3}H]Nitrendipine	Rat cerebral cortex	>30
Phenylalkylamine	[^{3}H](−)-D888	Rat brain	>30
N-type Ca^{2+} channel	^{125}I-ω-Conotoxin GVIA	Rat brain	>30
Na^+ channel			
Site 1	[^{3}H]Saxitoxin	Rat brain	>30
Site 2	[^{3}H]Batrachotoxinin	Rat brain	>30
K^+ channel			
K_A	^{125}I-Dendrotoxin	Rat cerebral cortex	>30
K_{ATP}	[^{3}H]Glyburide	Hamster beta cell	>30
K_V	^{125}I-Charybdotoxin	Rat brain	>30
SK_{Ca}	^{125}I-Apamin	Rat brain	>30

AMPA, α-amino-3-hydroxy-5-methyl-4-isoxazolepropionic acid; NMDA, *N*-methyl-D-aspartate; DPCPX, 8-cyclopentyl-1,3-dipropylxanthine; CGP-12177, 4-[3-[(1,1-dimethylethyl)amino]-2-hydroxypropoxy]-1,3-dihydro-2H-benzimidazol-2-one; CGS-21680, 2-*p*-(2-carboxyethyl)phenethylamino-5′-*N*-ethylcarboxamidoadenosine; AB-MECA, 4-aminobenzyl-5′-*N*-methylcarboxamidoadenosine; CGP-39653, (*E*)-2-amino-4-propyl-5-phosphono-3-pentenoic acid; D888, desmethoxyverapamil.

influx) by NCX much more effectively than the forward mode (Iwamoto et al., 1996, 2004; Elias et al., 2001). In addition, KB-R7943 is 3-fold more effective on NCX3 than on NCX1 and NCX2 (Iwamoto et al., 2001), whereas SEA0400 predominantly blocks NCX1 compared with NCX2 and NCX3 (Iwamoto et al., 2004). From mutational analyses, we have found that Gly833 in NCX1 is a common molecular determinant required for inhibition by KB-R7943 and SEA0400, whereas Phe213 is a specific determinant corresponding to inhibition by SEA0400 (Iwamoto et al., 2001, 2004). At present, KB-R7943 and SEA0400 are widely used as pharmacological tools to study the roles of the exchanger at the cellular and organ levels. For example, both NCX inhibitors have been shown to efficiently guard against toxicity by ischemia/reperfusion injury of the heart (Nakamura et al., 1998; Elias et al., 2001; Takahashi et al., 2003), kidney (Ogata et al., 2003; Yamashita et al., 2003), and brain (Matsuda et al., 2001).

We have developed SN-6, a new selective NCX inhibitor quite recently (Iwamoto et al., 2002). This drug (Fig. 1) was found by screening newly synthesized benzyloxyphenyl derivatives for inhibition of Na^+_i-dependent $^{45}Ca^{2+}$ uptake into NCX1-transfected fibroblasts. SN-6 has been reported to exhibit effective protective effects on the ischemia/reperfusion-injured heart by the dual actions of NCX inhibition and scavenging oxygen radicals (Hotta et al., 2002). Thus, SN-6 is expected to be a novel anti-ischemic drug. In this study, we investigated the inhibitory properties of SN-6 by measuring Na^+_i-dependent $^{45}Ca^{2+}$ uptake and searched for the structural domains responsible for its inhibition using chimeric analysis and subsequent site-directed mutagenesis. We identified critical amino acid residues in the XIP region, the substitution of which alters the apparent affinity of the drug.

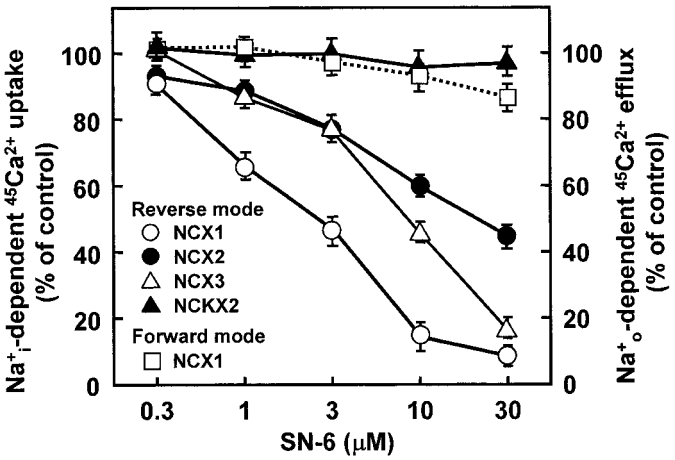

Fig. 2. Dose-response curves for the effects of SN-6 on Na^+_i-dependent $^{45}Ca^{2+}$ uptake (reverse mode) or Na^+_o-dependent $^{45}Ca^{2+}$ efflux (forward mode) in cells expressing NCX1, NCX2, NCX3, or NCKX2. The initial rates of $^{45}Ca^{2+}$ uptake into cells and $^{45}Ca^{2+}$ efflux from cells equilibrated with $^{45}Ca^{2+}$ were measured in the presence or absence of indicated concentrations of SN-6 as described under *Materials and Methods*. The uptake rates into control transfectants were 14, 6.4, 8.6, and 3.2 nmol/mg/30 s for NCX1, NCX2, NCX3, and NCKX2, respectively. The basal uptake rate into untransfectants was 0.1 nmol/mg/30 s. The efflux rates from control NCX1 transfectants and untransfectants were 0.65 and 0.02 nmol/mg/20 s, respectively. SN-6 was added 5 min before the start of uptake or efflux measurement. Data are presented as a percentage of the control values obtained in the absence of SN-6; the lines simply connect the data points. Data are means ± S.E. of four independent experiments.

Materials and Methods

Cell Cultures. Chinese hamster lung fibroblasts (CCL39 cells) and their NCX transfectants were maintained in Dulbecco's modified Eagle's medium (DMEM) supplemented with 7.5% fetal calf serum (FCS), 50 U/ml penicillin, and 50 μg/ml streptomycin in a humidified incubator gassed with 5% CO_2/95% air at 37°C. Porcine tubular epithelial cells LLC-PK_1 and their NCX transfectants were grown in DMEM supplemented with 4% FCS, 50 U/ml penicillin, and 50 μg/ml streptomycin.

Construction and Stable Expression of Wild-Type, Chimeric, and Mutant Exchangers. We used major splice variants of cDNAs for NCXs that are prevalent in dog hearts (NCX1.1) and rat brains (NCX2.1 and NCX3.3). NCX cDNAs were cloned into SacII and HindIII restriction sites in pCRII (Invitrogen, Carlsbad, CA) (Iwamoto et al., 1998). NCX1/NCX3 chimeras shown in Fig. 3 were constructed as described in detail previously (Iwamoto et al., 1999b, 2004). Substitution of amino acid residues in NCX1 was performed by site-directed mutagenesis using a polymerase chain reaction-based strategy as described previously (Iwamoto et al., 1999b). Successful construction of the modified cDNAs was verified by sequencing (ABI PRISM 3100 Genetic Analyzer; Applied Biosystems, Foster City, CA). These cDNAs were transferred into SacII and HindIII sites in the mammalian expression vector pKCRH. Rat NCKX2 cDNA was cloned into EcoRI and KpnI restriction sites in the mammalian expression vector pcDNA3.1 (Invitrogen), as described previously (Iwamoto et al., 2001). To obtain stable expression of wild-type, chimeric, and mutant exchangers, pKCRH or pcDNA3.1 plasmids carrying exchanger cDNAs were transfected in the presence of Lipofectin (Invitrogen) into CCL39 fibroblasts or LLC-PK_1 cells. Cell clones highly expressing NCX activity or NCKX activity were selected by a Ca^{2+}-killing procedure as described previously (Iwamoto et al., 1998).

Na^+_i-Dependent $^{45}Ca^{2+}$ Uptake into Cells. Na^+_i-dependent $^{45}Ca^{2+}$ uptake into cells expressing the wild-type or mutated exchangers were assayed as described in detail previously (Iwamoto et al., 2001). In brief, confluent transfectants in 24-well dishes were loaded with Na^+ by incubation at 37°C for 40 min in 0.5 ml of balanced salt solution (BSS) (10 mM HEPES/Tris, pH 7.4, 146 mM NaCl, 4 mM KCl, 2 mM $MgCl_2$, 0.1 mM $CaCl_2$, 10 mM glucose, and 0.1% bovine serum albumin) containing 1 mM ouabain and 10 μM monensin. $^{45}Ca^{2+}$ uptake was then initiated by switching the medium to Na^+-free BSS (replacing NaCl with equimolar choline chloride) or to normal BSS, both of which contained 0.1 mM $^{45}CaCl_2$ (370 kBq/ml) and 1 mM ouabain. After a 30-s incubation, $^{45}Ca^{2+}$ uptake was terminated by washing cells four times with an ice-cold solution containing 10 mM HEPES/Tris, pH 7.4, 120 mM choline chloride, and 10 mM $LaCl_3$. Cells were then solubilized with 0.1 N NaOH, and aliquots were taken for determination of radioactivity and protein. When present, SN-6 and KB-R7943 were included in the medium 15 min before the start of $^{45}Ca^{2+}$ uptake.

Na^+_o-Dependent $^{45}Ca^{2+}$ Efflux from Cells. $^{45}Ca^{2+}$ efflux from NCX1 transfectants cultured in a 35-mm dish was assayed as described previously (Iwamoto et al., 1996). Cells were equilibrated with $^{45}Ca^{2+}$ by incubating them at 37°C for 4 h in 1 ml of BSS containing 740 kBq of $^{45}Ca^{2+}$. After rinsing cells six times with Ca^{2+}- and Na^+-free BSS for 1 min, $^{45}Ca^{2+}$ efflux was measured for 20 s in Ca^{2+}- and Na^+-free BSS or in Ca^{2+}-free BSS; both solutions contained 1 μM thapsigargin to cause a transient increase in Ca^{2+}_i concentration. Na^+_o-dependent $^{45}Ca^{2+}$ efflux was estimated by subtracting $^{45}Ca^{2+}$ efflux in Ca^{2+}- and Na^+-free BSS from that in Ca^{2+}-free BSS.

Assay of Na^+_i-Dependent $^{45}Ca^{2+}$ Uptake into Sarcolemmal Vesicles. Na^+_i-dependent Ca^{2+} uptake into sarcolemmal vesicles, which were prepared from dog ventricular muscle, was measured essentially as described previously (Iwamoto et al., 1996). In brief, 5 μl of Na^+-loaded vesicles (1–2 mg/ml) was rapidly diluted into 0.25 ml of uptake medium [20 mM MOPS/Tris, pH 7.4, 160 mM KCl, 10

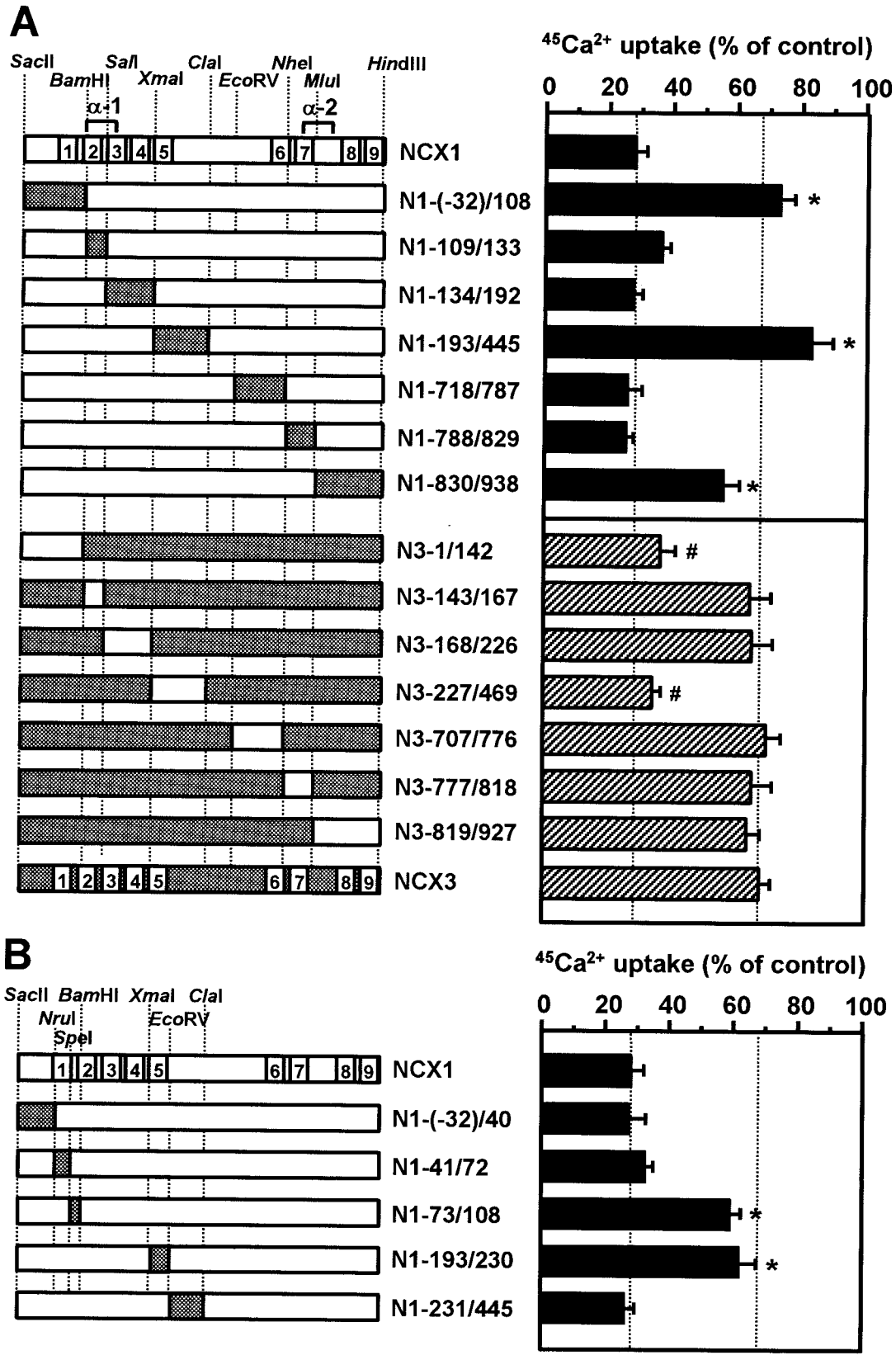

Fig. 3. Effects of SN-6 on Na^+_i-dependent $^{45}Ca^{2+}$ uptake into cells expressing chimeric exchangers between NCX1 and NCX3. A, two series of chimeras (N1 and N3) were constructed by substituting segments of NCX1 with homologous segments of NCX3 and vice versa. B, the second series of chimeras were constructed within SacII/BamHI and XmaI/ClaI regions. Chimeras are named from the amino acid numbers for their respective isoforms. The restriction enzyme cut sites are shown by broken lines, and the segments substituted with each other are indicated by ▧ or ■. Linear models of the exchangers are indicated at the top and/or bottom, and the numbered open boxes show positions of transmembrane segments. The initial rates of $^{45}Ca^{2+}$ uptake into cells were measured in the presence or absence of 5 μM SN-6. The uptake rates in cells expressing N1 or N3 chimeras were 10 to 15 and 4 to 9 nmol/mg/30 s, respectively. Data are means ± S.E. of four independent experiments. ★, $p < 0.05$ versus NCX1; #, $p < 0.05$ versus NCX3.

μM $^{45}CaCl_2$ (10 kBq), and 0.5 μM valinomycin] at 37°C. The reaction was stopped at 1.5 s by adding 4 ml of ice-cold washing medium (160 mM KCl and 1 mM $LaCl_3$). Vesicles were collected on a glass fiber filter and washed twice with the same medium. Blanks were obtained by measuring $^{45}Ca^{2+}$ uptake in medium containing NaCl instead of KCl. These blanks were subtracted from all data points to correct for Na^+-independent $^{45}Ca^{2+}$ uptake.

Assays of Various Receptors, Ion Transporters, and Ion Channels. The binding assays to receptors and ion channels (Table 1) were performed by MDS Pharma Services (Taipei, Taiwan). The binding activity to the muscarinic acetylcholine receptor was determined using [^{3}H]L-quinuclidinyl benzilate (QNB) (Luthin and Wolfe, 1984). The activities of ion transporters, such as the Na^+/H^+ exchanger, the Na^+,K^+-ATPase, and Ca^{2+}-ATPases, were measured as described previously (Iwamoto et al., 1996).

Hypoxia and Reoxygenation in LLC-PK$_1$. LLC-PK$_1$ and their NCX transfectants were grown in 96-well microplates at 2×10^5 cells/well. After 2 days, the medium was changed to HEPES-buffered DMEM without glucose and FCS. The cells were exposed to hypoxic conditions in an Anaero Pack Pouch (Mitsubishi Gas Chemical, Tokyo, Japan), in which the oxygen concentration was less than 1% within 1 h, as described previously (Iwamoto et al., 2004). After 6 h of hypoxia, the cells were put in a humidified incubator gassed with 5% CO_2/95% air for 1 h in HEPES-buffered DMEM to which glucose was added at the beginning of reoxygenation. After the hypoxia/reoxygenation treatment, lactate dehydrogenase (LDH) activity in the medium was measured using an LDH-Cytotoxic Test kit (Wako Pure Chemicals, Osaka, Japan). SN-6 (0.3–10 μM) was added to the medium at the beginning of reoxygenation. LDH release was expressed as a percentage of total cellular LDH activity.

Assay of ATP Content. For ATP measurement, cells (5×10^6 cells/35-mm dish) were extracted with ice-cold 8% perchloric acid, and the extract was then neutralized with 1 M Tris. The ATP concentration was assayed by the luciferin-luciferase method (ATP Bioluminescence Assay Kit; Roche Diagnostics, Indianapolis, IN).

Statistical Analysis. Data are expressed as means ± S.E. of three or four independent determinations. IC_{50} values for $^{45}Ca^{2+}$ uptake, ligand binding, and cell damage were calculated by nonlinear least-squares fits using the program Prism (GraphPad Software Inc., San Diego, CA). Differences for multiple comparisons were analyzed by an unpaired t test or one-way analysis of variance followed by Dunnett's test. Values of $p < 0.05$ were considered statistically significant.

Materials. CCL39 and LLC-PK$_1$ were purchased from American Type Culture Collection (Manassas, VA). SN-6 was synthesized by Senju Pharmaceutical Co. Ltd. (Kobe, Japan). KB-R7943 was provided by Nippon Organon (Osaka, Japan). $^{45}CaCl_2$ and [^{3}H]QNB were purchased from Amersham Biosciences Inc. (Piscataway, NJ). XIP (RRLLFYKYVYKRYRAGKQRG) and V9M,Y10H (RRLLFYKYM-HKRYRAGKQRG) were synthesized by the Peptide Institute (Osaka, Japan). All other chemicals were also of the highest grade available.

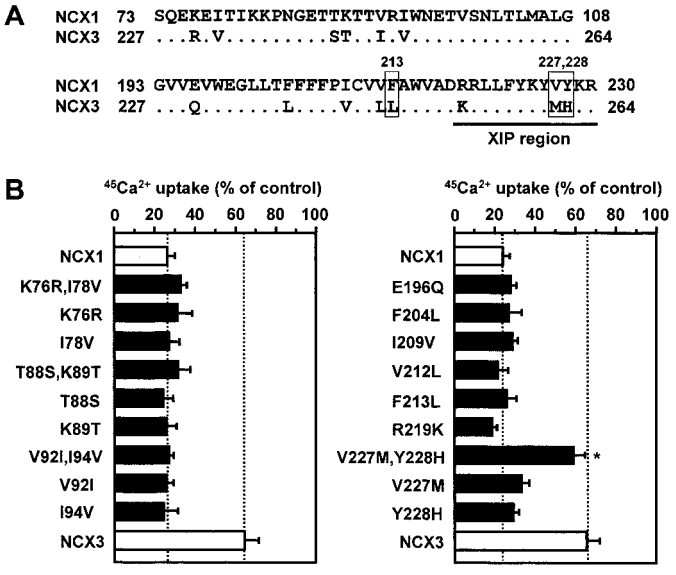

Fig. 4. Amino acid residues involved in drug sensitivity. A, amino acid alignment of regions responsible for drug sensitivity (positions 73–108 and 193–230 of NCX1) in NCX1 and NCX3. Conserved amino acids between exchangers are indicated with dots. The box shows the amino acid position of NCX1 and NCX3 whose mutation alters the SN-6 sensitivity. B, effects of SN-6 on Na^+_i-dependent $^{45}Ca^{2+}$ uptake into cells expressing NCX1 mutants substituted at their unique residues. The unique residues in regions indicated in A were exchanged to the corresponding residue of NCX3. The initial rates of $^{45}Ca^{2+}$ uptake were measured in the presence or absence of 5 μM SN-6. The uptake rates in cells expressing these mutants were 6 to 13 nmol/mg/30 s. Data are presented as a percentage of the values obtained in the absence of the drug. Data are presented as means ± S.E. of four independent experiments. ★, $p <$ 0.05 versus NCX1.

Results

Inhibitory Properties of SN-6. We first compared the inhibitory effects of SN-6 on Na^+_i-dependent $^{45}Ca^{2+}$ uptake into CCL39 cells with a stable transfection of NCX isoforms (NCX1, NCX2, and NCX3) or K^+-dependent Na^+/Ca^{2+} exchanger (NCKX2). SN-6 (up to 30 μM) inhibited dose-dependently the initial rate of $^{45}Ca^{2+}$ uptake into NCX1, NCX2, and NCX3 transfectants with IC_{50} values of 2.9 ± 0.12, 16 ± 1.1, and 8.6 ± 0.27 μM ($n = 3$), respectively, but it did not significantly affect uptake into NCKX2 transfectants (Fig. 2), indicating that SN-6 has a selectivity to NCX1. To check whether SN-6 competes with extracellular Ca^{2+} (Ca^{2+}_o) for the exchanger, the rate of Na^+_i-dependent $^{45}Ca^{2+}$ uptake into NCX1 transfectants was measured under standard conditions as a function of Ca^{2+}_o concentration (0.06–2 mM) in the presence or absence of 3 μM SN-6. Their double reciprocal plots of uptake rate versus Ca^{2+}_o concentration were linear (data not shown). SN-6 increased the half-maximal Ca^{2+} concentration value from 0.19 ± 0.02 mM of the control to 0.36 ± 0.03 mM ($p < 0.05$, $n = 3$) and decreased the corresponding V_{max} value from 26 ± 1.8 nmol/mg/30 s of the control to 12 ± 1.1 nmol/mg/30 s ($p < 0.05$), suggesting a type of mixed (competitive and noncompetitive) inhibition.

We next examined the effects of SN-6 on Na^+_o-dependent $^{45}Ca^{2+}$ efflux from NCX1 transfectants equilibrated with $^{45}Ca^{2+}$ and treated with 1 μM thapsigargin. The rate of Na^+_o-dependent $^{45}Ca^{2+}$ efflux was estimated by subtracting $^{45}Ca^{2+}$ efflux in a Ca^{2+}- and Na^+-free medium from that in a Ca^{2+}-free medium containing 146 mM Na^+. As shown in Fig. 2, SN-6 at 0.3 to 30 μM did not affect the rate of Na^+_o-dependent $^{45}Ca^{2+}$ efflux (i.e., the forward mode).

Selectivity of SN-6. We studied the effect of SN-6 on several receptors and ion channels using ligand-binding assays. SN-6 at 3 to 30 μM did not significantly affect the receptors and channels listed in Table 1, except for the muscarinic acetylcholine receptor ($IC_{50} = 18$ μM, $n = 3$). However, SN-6 at 3 μM, which is close to the IC_{50} value for NCX1, exhibited a minimal inhibition (6.1 ± 1.5%, $n = 3$) in the muscarinic acetylcholine receptor (i.e., [^{3}H]QNB binding). On the other hand, KB-R7943 at 4.5 μM, which approximates the IC_{50} value for NCX1, potently inhibited the muscarinic acetylcholine receptor by 84 ± 3.2% ($IC_{50} = 0.71$ μM, $n = 3$). SN-6 (up to 30 μM) did not significantly influence the

Na^+/H^+ exchanger, Na^+,K^+-ATPase, and sarcolemmal or sarcoplasmic reticulum Ca^{2+}-ATPase (data not shown).

Chimeric Analysis of the Inhibitory Effect of SN-6. Taking advantage of the fact that NCX1 and NCX3 differ from each other in their sensitivity to SN-6 despite their high sequence homology, we performed chimeric analysis between these isoforms to identify important region(s) in the NCX1 molecule for the interaction with SN-6 (Fig. 3). We constructed two series of chimeras in which serial segments from NCX3 were transferred into NCX1 in exchange for the homologous segments (N1 chimeras) and vice versa (N3 chimeras). N1 and N3 chimeras exhibited exchange activities similar to those of wild-type NCX1 and NCX3, respectively (see the legend to Fig. 3).

Figure 3A shows the effect of 5 μM SN-6 on the rate of Na^+_i-dependent $^{45}Ca^{2+}$ uptake into CCL39 cells expressing wild-type or chimeric exchangers. SN-6 at this concentration reduced the uptake rates of the wild-type NCX1 and NCX3 to approximately 30 and 70% of the control, respectively. In N1 chimeras, three chimeras, N1-(−32)/108, N1-193/445, and N1-830/938—which contained the homologous SacII/BamHI, XmaI/ClaI, and MluI/HindIII segments from NCX3, respectively—exhibited an SN-6 sensitivity similar to that of wild-type NCX3. On the other hand, N3 chimeras (N3-1/142 and N3-227/469) containing SacII/BamHI and XmaI/ClaI segments exhibited an SN-6 sensitivity similar to that of wild-type NCX1. Therefore, we focused on SacII/BamHI and XmaI/ClaI segments that displayed the reciprocal results in N1 and N3 chimeras and further analyzed the second series of chimeras (Fig. 3B), which were constructed by exchanging smaller segments within these two regions. Among an additional five chimeras, N1-73/108 and N1-193/230, which contained the homologous SpeI/BamHI (i.e., the first intracellular loop region) and XmaI/EcoRV segments (i.e., the fifth transmembrane region with part of the XIP region) from NCX3, showed significantly reduced sensitivities to inhibition by SN-6, which are nearly equivalent to those observed in wild-type NCX3.

Identification of Residues Involved in Drug Sensitivity. Figure 4A shows amino acid sequences of NCX1 and NCX3 in SpeI/BamHI (amino acids 73–108 in NCX1) and XmaI/EcoRV segments (amino acids 193–230 in NCX1), which contain six and eight residues, respectively, unique to each isoform. To identify the critical residues involved in drug sensitivity, these unique residues in NCX1 were exchanged with the corresponding residues in NCX3, one or two residues at a time. Nine mutants derived from the SpeI/BamHI region did not produce any significant change in sensitivity to inhibition by 5 μM SN-6 (Fig. 4B). On the other hand, among nine mutants derived from the XmaI/EcoRV region, only the V227M,Y228H double mutant exhibited a significantly decreased SN-6 sensitivity to a level almost comparable with that observed in wild-type NCX3, although the single mutants V227M and Y228H did not affect the drug sensitivity (Fig. 4B). The IC_{50} value for V227M,Y228H was 12 ± 0.72 μM ($n = 3$), which was approximately four times as large as that for wild-type NCX1 (Fig. 5).

We further analyzed the effects of SN-6 on critical NCX1 mutants that have been shown to exhibit a very low sensitivity to KB-R7943 or SEA0400 (Iwamoto et al., 2001, 2004). As shown in Fig. 5, SN-6, as well as KB-R7943, had almost no effect on Ca^{2+} uptake by G833C. It was remarkable that we found from screening NCX1 mutants newly constructed at residues neighboring Gly833 that N839A exhibited a markedly decreased sensitivity to inhibition by SN-6 or KB-R7943. On the other hand, SN-6 normally inhibited uptake by F213L, which is insensitive to SEA0400. In addition, we examined the effects of SN-6 on other multiple mutants, F213A, F213C, and F213R, and found that among them, SN-6 was least sensitive to only F213R (Fig. 5). KB-R7943 normally inhibited uptakes by all multiple mutants at Phe213 and by the V227M,Y228H mutant, the inhibition being equal to that by wild-type NCX1.

In Vitro Interaction of SN-6 with XIP Peptides. Because critical amino acids (Val227 and Tyr228) responsible for the inhibition by SN-6 were located in the XIP region (Fig.

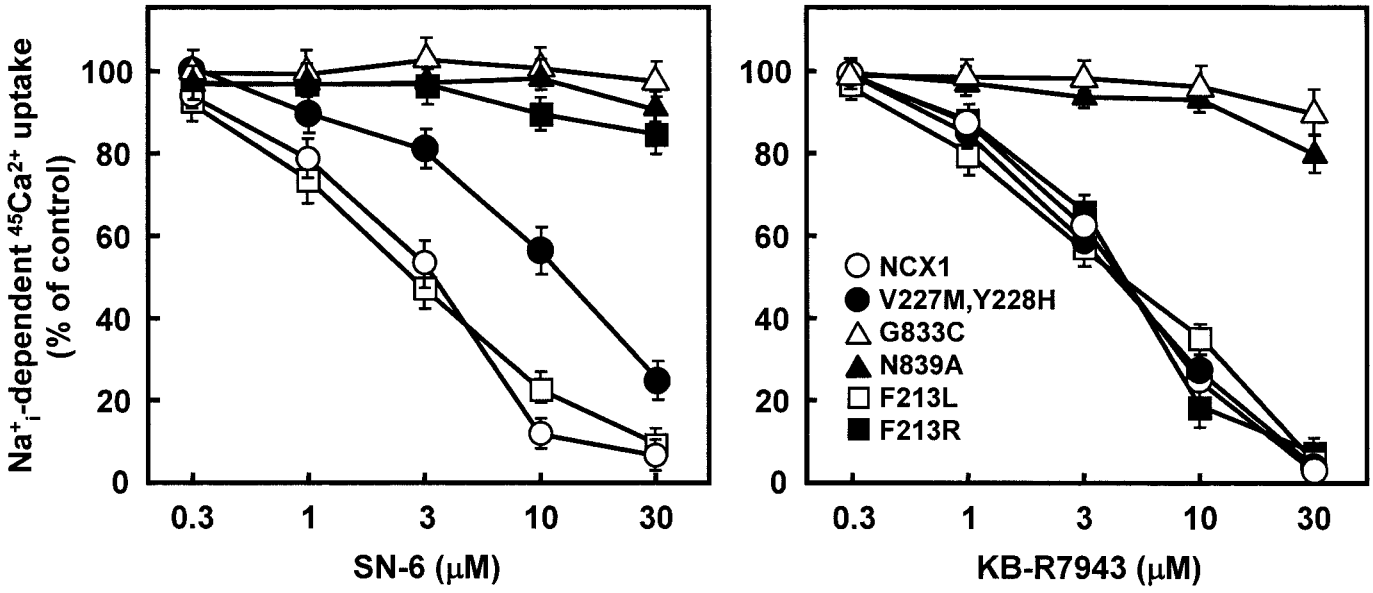

Fig. 5. Dose-response curves for the effects of SN-6 and KB-R7943 on Na^+_i-dependent $^{45}Ca^{2+}$ uptake into cells expressing wild-type NCX1 and several NCX1 mutants. The initial rates of $^{45}Ca^{2+}$ uptake were measured in the presence or absence of indicated concentrations of drugs. Data are means ± S.E. of three independent experiments.

4A), we analyzed the interaction of SN-6 with synthesized XIP peptides by measuring Na^+_i-dependent $^{45}Ca^{2+}$ uptake into cardiac sarcolemmal vesicles. SN-6 (0.3–30 μM) completely and dose-dependently inhibited the initial rate of Na^+_i-dependent $^{45}Ca^{2+}$ uptake into Na^+-loaded sarcolemmal vesicles (IC_{50} = 5.3 ± 0.37 μM, n = 3) (Fig. 6A). On the other hand, wild-type XIP and XIP peptide with double substitutions V9M,Y10H (0.1–10 μM), which are in homologous positions to Val227 and Tyr228 in NCX1, equally and incompletely (approximately 60%) blocked the uptake. As shown in Fig. 6B, SN-6 exhibited the same inhibitory efficacy in $^{45}Ca^{2+}$ uptake into vesicles even in the presence of 1 μM XIP (IC_{50} = 4.9 ± 0.53 μM, n = 3) or V9M,Y10H peptide (5.5 ± 0.28 μM, n = 3).

I_1 Inactivation- and ATP Depletion-Dependent Inhibition by SN-6. We analyzed the effects of SN-6 on NCX1 mutants which display the altered kinetics of Na^+-dependent inactivation (i.e., I_1 inactivation). XIP region mutants K229Q and F223E have been shown to exhibit completely eliminated and enhanced I_1 inactivation, respectively (Matsuoka et al., 1997; Iwamoto et al., 2004). As shown in Fig. 7, K229Q and F223E mutants exhibited a markedly reduced sensitivity and hypersensitivity, respectively, to inhibition by SN-6. In addition, we examined the effects of ATP depletion on the inhibition by SN-6 in wild-type NCX1 and in K229Q and F223E mutants. Treatment with 2.5 μg/ml oligomycin and 10 mM 2-deoxy-D-glucose for 20 min markedly reduced cell ATP contents to less than 5% of control in NCX1, K229Q, and F223E transfectants. Such ATP depletion decreased the $^{45}Ca^{2+}$ uptake via NCX1 by approximately 30%, consistent with previously reported results (Iwamoto et al., 1998), but did not significantly decrease that via K229Q or F223E. The dose-response curve for inhibition by SN-6 obtained in ATP-depleted NCX1 transfectants was intriguingly shifted to the left compared with that obtained in the control cells (Fig. 7). The IC_{50} value (0.78 ± 0.11 μM, n = 3) of the former was approximately one fourth that of the latter. On the other hand, cell ATP depletion did not significantly affect the inhibition by SN-6 in K229Q and F223E transfectants.

Effect of SN-6 on Renal Hypoxia/Reoxygenation-Induced Injury. We examined the renoprotective effect of SN-6 in hypoxia/reoxygenation-induced injury in LLC-PK_1 cells derived from porcine proximal tubules. In parental LLC-PK_1 cells, 6 h of hypoxia followed by 1 h of reoxygenation produced a significant LDH release from damaged cells (Fig. 8). The hypoxia/reoxygenation-induced LDH release was 2.4- to 2.8-fold enhanced in LLC-PK_1 cells overexpressing wild-type NCX1 or K229Q mutant. In these transfectants, the expression levels of exchangers were 250 to 300% higher than the endogenous NCX1 protein, judging from immunoblot analysis (data not shown). SN-6 (0.3–10 μM) dose-dependently protected against the hypoxia/reoxygenation-induced LDH release in parental LLC-PK_1 cells and NCX1 transfectants but not in K229Q transfectants (Fig. 8). In NCX1 transfectants, the IC_{50} value of SN-6 for hypoxia/reoxygenation-induced LDH release was 0.63 ± 0.15 μM (n = 3) (the maximal inhibition was defined by the value obtained at 10 μM.).

Discussion

Organic NCX inhibitors are being developed as a pharmacological tool for the study of NCX's physiological role and function or as a new remedy for ischemic disease, arrhythmia, hypertension, and so on. In this study, we investigated the properties and molecular determinants of NCX inhibition by SN-6, a newly synthesized benzyloxyphenyl derivative, mainly by measuring the Na^+_i-dependent $^{45}Ca^{2+}$ uptake into CCL39 fibroblasts stably expressing NCX isoforms, NCX1/NCX3 chimeras, and site-directed NCX1 mutants. We show here that SN-6 is a unique NCX inhibitor and structural domains responsible for its inhibition may exist close to the endogenous XIP region.

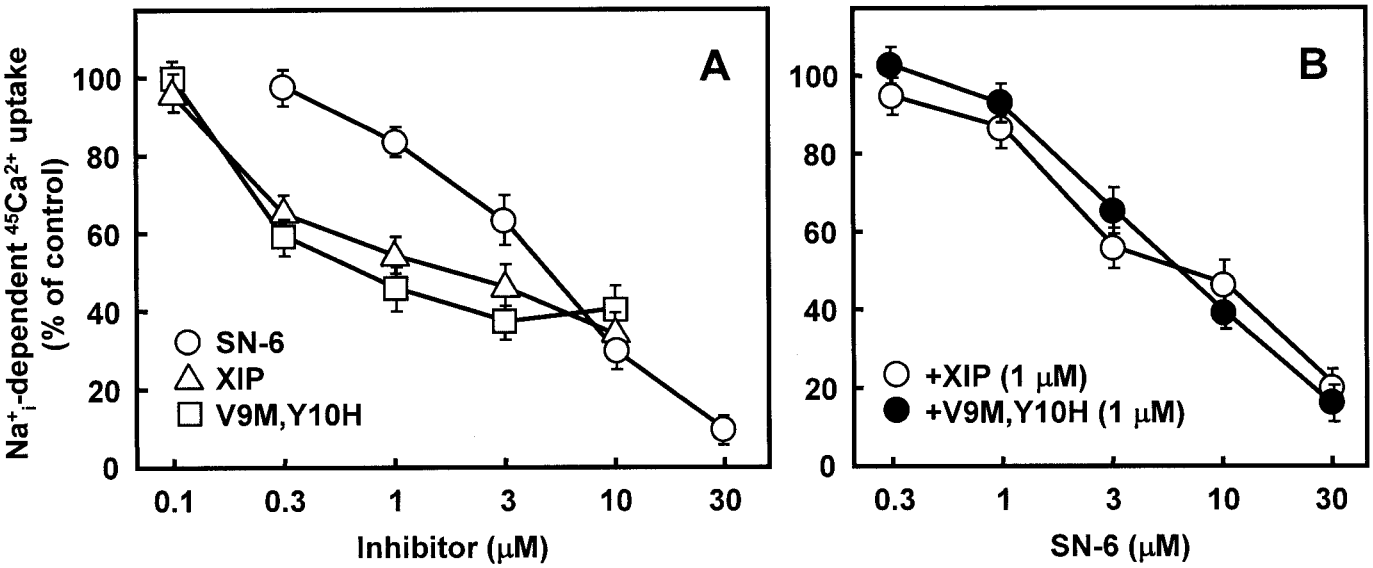

Fig. 6. Inhibition of Na^+/Ca^{2+} exchange by SN-6 or XIP peptides in sarcolemmal vesicles. A, the initial rates of Na^+_i-dependent $^{45}Ca^{2+}$ uptake into cardiac sarcolemmal vesicles were measured in the presence or absence of indicated concentrations of SN-6, wild-type XIP, and V9M,Y10H peptides as described under *Materials and Methods*. The uptake rates into control vesicles were 22 nmol/mg/1.5 s. The data are presented as a percentage of the control value. B, effects of SN-6 on Na^+_i-dependent $^{45}Ca^{2+}$ uptake into vesicles were measured in the presence of 1 μM XIP or 1 μM V9M,Y10H. The data are presented as a percentage of control values obtained in the absence of SN-6. Data are means ± S.E. of three independent experiments.

Properties of SN-6. Our study using transfectants expressing the NCX family revealed that SN-6 inhibits $^{45}Ca^{2+}$ uptake by NCX1 (IC_{50} = 2.9 μM) 3- to 5-fold more potently than that by NCX2 or NCX3, but not that by NCKX2 (Fig. 2). We reported previously that the isoform selectivity of other benzyloxyphenyl derivatives: KB-R7943 is 3-fold more inhibitory to NCX3 than to NCX1 and NCX2, whereas SEA0400 predominantly blocks NCX1, only mildly blocks NCX2, and exerts almost no influence on NCX3 (Iwamoto et al., 2001, 2004). Thus, SN-6 exhibits a different type of isoform selectivity among benzyloxyphenyl derivatives. Because the chemical structures of SN-6 and KB-R7943 (Fig. 1) differ only in the substituent of phenyl moiety, these substituents seem to be important for selectively sensing NCX1 and NCX3 isoforms, respectively. Thereafter, to evaluate the transport mode selectivity, we measured the effect of SN-6 on the Na^+_o-dependent $^{45}Ca^{2+}$ efflux (i.e., the forward mode) from NCX1 transfectants (Fig. 2). SN-6 (0.3–30 μM) did not significantly affect the $^{45}Ca^{2+}$ efflux, suggesting that this drug possesses selectivity for the reverse mode. Such mode selectivity is a common feature in other benzyloxyphenyl derivatives (see Introduction), although its mechanism is unknown at present.

We further examined the general specificity of SN-6 action. SN-6 (up to 30 μM) did not significantly affect several receptors, ion channels, and other transporters (see *Results*), with the exception of the muscarinic acetylcholine receptor (IC_{50} = 18 μM). It has previously been reported that KB-R7943 at the same dose for NCX inhibition inhibits acetylcholine receptors, the *N*-methyl-D-aspartate receptor, L-type Ca^{2+}-channel sites, and the Na^+-channel site (Sobolevsky and Khodorov, 1999; Pintado et al., 2000; Matsuda et al., 2001). We also confirmed that KB-R7943 potently inhibited [^{3}H]QNB binding for the muscarinic acetylcholine receptor (IC_{50} = 0.71 μM). Therefore, SN-6 is a more selective NCX inhibitor than KB-R7943.

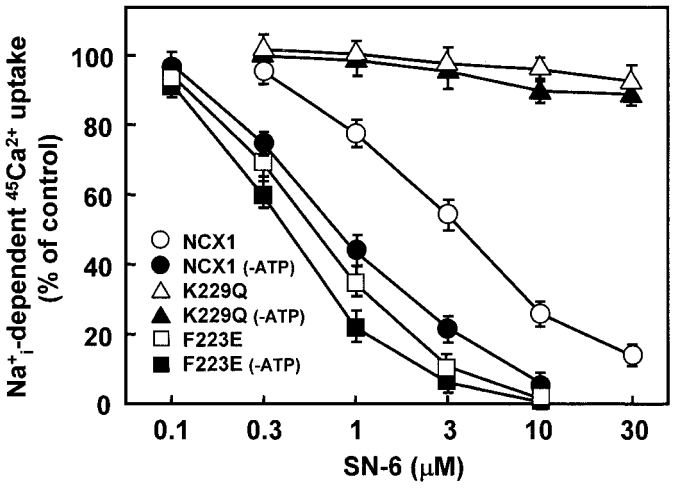

Fig. 7. Effects of ATP depletion on the inhibition of Na^+_i-dependent $^{45}Ca^{2+}$ uptake by SN-6 in cells expressing wild-type NCX1 and K229Q and F223E mutants. The initial rates of $^{45}Ca^{2+}$ uptake into cells were measured in the presence or absence of indicated concentrations of SN-6 as described under *Materials and Methods*. The uptake rates into control transfectants were 13, 17, and 7.3 nmol/mg/30 s for NCX1, K229Q, and F223E, respectively. Cells were pretreated with 10 mM D-glucose (control) or 2.5 μg/ml oligomycin and 10 mM 2-deoxy-D-glucose (-ATP) during the last 20 min of Na^+ loading. Data are means ± S.E. of three independent experiments.

Structural Domains for NCX1 Inhibition by SN-6. As suggested above, SN-6 is 3-fold more effective in inhibiting NCX1 than NCX3. Taking advantage of this property, we used a chimera strategy to identify critical region(s) of the exchanger involved in the differential response to SN-6. Phased series of analyses with NCX1/NCX3 chimeras revealed that amino acid regions 73 to 108 and 193 to 230 of NCX1 were primarily responsible for the difference in drug sensitivity between NCX1 and NCX3 (Fig. 3). These two regions primarily correspond to the first intracellular loop, and the fifth transmembrane and part of the XIP region, respectively. To further identify critical residues within these regions, the unique amino acids in NCX1 were substituted individually or in combination with those of NCX3 (Fig. 4). Thereafter, we found that double substitutions V227M,Y228H significantly reduce the drug sensitivity to a level almost comparable with that observed in the wild-type NCX3. On the other hand, single substitution V227M or Y228H did not affect the drug sensitivity, suggesting that the continuous residues Val227 and Tyr228 are cooperatively involved in the sensitivity to SN-6.

Because both residues are located in the XIP region, we further analyzed the interaction of SN-6 with both the wild-type XIP peptide and the V9M,Y10H mutant in $^{45}Ca^{2+}$ uptake assay using cardiac sarcolemmal vesicles (Fig. 6). It was unfortunate that we could not detect the in vitro interaction of SN-6 with XIP peptides. However, it is difficult to interpret the failure of SN-6 to affect XIP peptide inhibition in connection with the inhibitory action of SN-6 because the interaction mechanism between endogenous XIP function and synthesized XIP peptides is unknown. Indeed, because multiple residues (see below) contribute to the inhibitory action of SN-6, there is a possibility that only the XIP peptide containing Val227 and Tyr228 residues cannot interact with SN-6. Phosphatidylinositol-4,5-bisphosphate has recently been reported to directly interact with the XIP region and to regulate I_1 inactivation (Philipson and Nicoll, 2000). Therefore, to assess the interaction between SN-6 and the endogenous XIP region, it seems to be necessary to electrophysiologically ex-

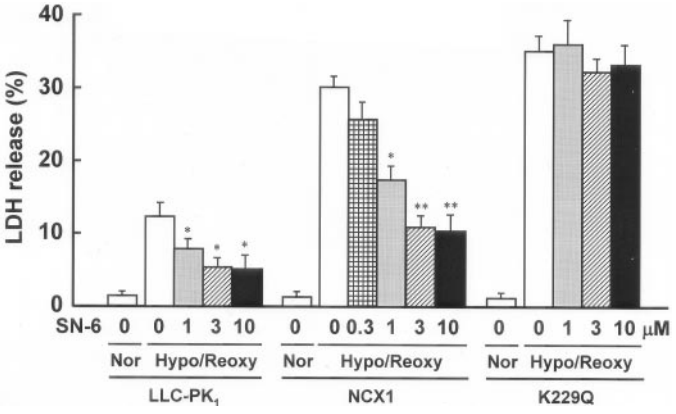

Fig. 8. Effects of SN-6 on the LDH release induced by hypoxia/reoxygenation in LLC-PK_1 cells expressing the wild-type NCX1 or K229Q mutant. Cells were exposed to 7 h of normoxia (Nor) or 6 h of hypoxia followed by 1 h of reoxygenation (Hypo/Reox). SN-6 (0.3–10 μM) was added to the culture medium during the last 1 h of reoxygenation. Data are means ± S.E. of five independent experiments. LDH release is expressed as a percentage of total cellular LDH activity. ★, $p < 0.05$; ★★, $p < 0.01$ versus hypoxia/reoxygenation without SN-6.

amine the effect of SN-6 on phosphatidylinositol-4,5-bisphosphate–induced exchange activation using the inside-out patch from cells overexpressing NCX1 or XIP mutants.

To evaluate the interaction of SN-6 with molecular determinants for NCX1 inhibition by KB-R7943 or SEA0400, we examined the effects of SN-6 on NCX1 mutants G833C and F213L, of which G833C is insensitive to both inhibitors and F213L is insensitive to SEA0400 (Iwamoto et al., 2001, 2004). SN-6 as well as KB-R7943 exhibited undetectable effects on G833C, whereas this drug showed the same inhibitory effect on F213L as on the wild-type NCX1. However, we found from multiple mutants at Phe213 that only F213R was insensitive to SN-6. In addition, we discovered that N839A mutant was insensitive to SN-6 and KB-R7943 by screening mutants newly constructed at residues neighboring Gly833. On the other hand, KB-R7943 normally blocked V227M,Y228H and F213R mutants. Therefore, we suppose that the XIP region (containing Val227 and Tyr228) and its neighboring regions such as the fifth transmembrane (containing Phe213) and the α-2 repeat (containing Gly833 and Asn839) may participate in the formation of the interaction domains with SN-6, as illustrated in Fig. 9.

On the other hand, we found that the inhibitory effect of SN-6 is connected with I_1 inactivation (see below). It suggests the possibility that critical mutants (V227M,Y228H, F213R, G833C, and N839A), which display reduced sensitivities to SN-6, have altered the kinetics of I_1 inactivation. We confirmed that V227M,Y228H, F213R, and G833C mutants displayed apparently normal I_1 inactivation by measuring whole-cell outward exchange currents, although we could not evaluate the N839A mutant because of its unstable expression (A. Uehara and T. Iwamoto, unpublished observations). In addition, with respect to V227M,Y228H and F213R mutants, their reduced drug sensitivities were detected in inhibition by SN-6 but not in that by KB-R7943 (Fig. 5). These specificities to SN-6 support the assumption that the effects on these mutants, unlike K229Q, are not caused by the altered I_1 inactivation. Thus, at least V227M,Y228H, F213R, and G833C mutations seem to be directly interfering with the drug binding rather than affecting the I_1 inactivation (Fig. 9).

I_1 Inactivation- and ATP Depletion-Dependent Inhibition by SN-6. NCX is controlled by inactivation processes such as I_1 and I_2 inactivation (see Introduction). Matsuoka et al. (1997) reported previously that XIP region mutants had drastically altered I_1 inactivation kinetics, suggesting that the XIP region is involved in the I_1 inactivation process. Among the XIP region mutants, K229Q and F223E displayed distinctive features, namely loss of or marked acceleration, respectively, of I_1 inactivation. To explore the possible link between the inhibition by SN-6 and I_1 inactivation, we examined the effect of SN-6 on $^{45}Ca^{2+}$ uptake by K229Q and F223E. SN-6 was not effective in inhibiting the uptake by K229Q, whereas this drug exhibited significant hypersensitivity to F223E compared with wild-type NCX1 (Fig. 7). These data suggest that the inhibitory effect of SN-6 is related to the kinetics of I_1 inactivation. Similar results have also been observed in other benzyloxyphenyl derivatives, including KB-R7943 and SEA0400 (Bouchard et al., 2004; Iwamoto et al., 2004). K229Q apparently works as a constitutively active exchanger, as do Y224W/Y226W/Y228W/Y231W (termed XIP-4YW) and Δ229–232, which were used in the above-cited reports. These mutants hardly seem to enter the I_1 inactive state. The marked reduction of drug

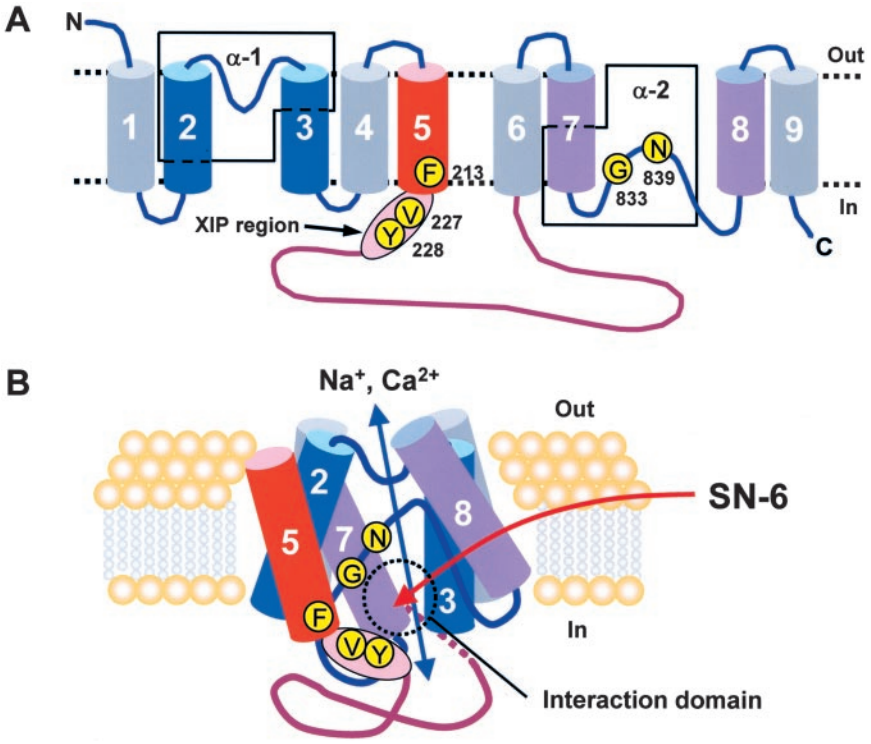

Fig. 9. Putative interaction domains for SN-6 in NCX1. A, a nine-transmembrane model of NCX1 taken from recent topology analyses (Iwamoto et al., 1999a; Nicoll et al., 1999). The amino acid residues of NCX1 whose mutation alters the sensitivity to SN-6 are indicated. B, illustration representing the imagined structural domains responsible for SN-6. The indicated helix packing of transmembrane segments 2, 3, 7, and 8 is suggested by cross-linking data (Qiu et al., 2001).

sensitivity in these mutants suggests that benzyloxyphenyl derivatives may specifically target the I_1 inactive state. This possibility received support from the evidence that benzyloxyphenyl derivatives had hypersensitivities to N1-F223E, which are able to very quickly enter an I_1 inactive state (Bouchard et al., 2004; Iwamoto et al., 2004). Therefore, we speculate that the interaction of benzyloxyphenyl derivatives with the exchanger probably stabilizes the I_1 inactive state or accelerates the rate of entry into an I_1 inactive state.

Cellular ATP regulates the NCX function (Haworth et al., 1987; Hilgemann et al., 1992a; Condrescu et al., 1995; Iwamoto et al., 1998). We then examined the effects of ATP depletion on the inhibition by SN-6 in fibroblasts expressing the wild-type NCX1 and K229Q and F223E mutants. ATP depletion (down to less than 5% of control level) produced a partial decrease in the basal activity of NCX1 but not in that of K229Q or F223E. It was intriguing that in ATP-depleted NCX1 transfectants, the sensitivity to inhibition by SN-6 was enhanced, whereas there was no change in ATP-depleted K229Q or F223E transfectant (Fig. 7). Such ATP depletion-induced drug hypersensitivity seems to be related to the I_1 inactivation process, although ATP depletion is known to affect many aspects of cell metabolism (Hilgemann, 1997).

Renoprotective Effects of SN-6. SN-6 has been shown to efficiently guard against ischemia/reperfusion injury in perfused guinea pig Langendorff hearts (Hotta et al., 2002). This simply suggests that during reperfusion resulting in cardiac dysfunction and cell damage, SN-6 blocks Ca^{2+} overload primarily via NCX. However, the quality of this interpretation depends on the real selectivity of SN-6. Therefore, we verified its pharmacological efficacy based on the inhibition of the exchanger by SN-6 using the SN-6-insensitive mutant K229Q. We performed hypoxia/reoxygenation-induced injury in LLC-PK_1 cells derived from porcine proximal tubules as a model experiment. SN-6 significantly protected against hypoxia/reoxygenation-induced cell damage in parental and NCX1-transfected LLC-PK_1 cells but not in K229Q-transfected cells (Fig. 8). These results suggest that the inhibition of the exchanger by SN-6 is sure to be participating in its renoprotective effect.

Ischemia followed by reperfusion in several organs generally depletes cellular ATP. We confirmed that LLC-PK_1 cells exposed to 6-h hypoxia had cellular ATP content reduced to less than 5% of control level. As a result, in our hypoxia/reoxygenation study, SN-6 seemed to act on the exchanger under ATP-depleted conditions. Under these conditions, SN-6 potently blocked hypoxia/reoxygenation-induced injury in NCX1-transfected LLC-PK_1 with an IC_{50} value of 0.63 μM. This IC_{50} value is smaller than that for the inhibition of NCX1 in normal NCX1 transfectants (IC_{50} = 2.9 μM), being almost equivalent to that for the inhibition of NCX1 in the ATP-depleted cells (IC_{50} = 0.78 μM). These results suggest that SN-6 predominantly works as a blocker of Ca^{2+} overload via NCX under hypoxic/ischemic conditions. Such a property of SN-6, which might be derived from its interaction with the endogenous XIP region, seems to be advantageous to developing it clinically as a new renal and cardiac protective anti-ischemic drug. Furthermore, this drug may be useful as a tool with which to study the I_1 inactivation and ion transport mechanisms of NCX.

Acknowledgments

We greatly appreciate our valuable discussions with Dr. M. Shigekawa (Senri Kinran College).

References

Bers DM (2002) Cardiac excitation-contraction coupling. *Nature (Lond)* **415:**198–205.

Blaustein MP and Lederer WJ (1999) Sodium/calcium exchange: its physiological implications. *Physiol Rev* **79:**763–854.

Bouchard R, Omelchenko A, Le HD, Choptiany P, Matsuda T, Baba A, Takahashi K, Nicoll DA, Philipson KD, Hnatowich M, et al. (2004) Effects of SEA0400 on mutant NCX1.1 Na^+-Ca^{2+} exchangers with altered ionic regulation. *Mol Pharmacol* **65:** 802–810.

Condrescu M, Gardner JP, Chernaya G, Aceto JF, Kroupis C, and Reeves JP (1995) ATP-dependent regulation of sodium-calcium exchange in Chinese hamster ovary cells transfected with the bovine cardiac sodium-calcium exchanger. *J Biol Chem* **270:**9137–9146.

Doering AE, Nicoll DA, Lu Y, Lu L, Weiss JN, and Philipson KD (1998) Topology of a functionally important region of the cardiac Na^+/Ca^{2+} exchanger. *J Biol Chem* **273:**778–783.

Elias CL, Lukas A, Shurraw S, Scott J, Omelchenko A, Gross GJ, Hnatowich M, and Hryshko LV (2001) Inhibition of Na^+/Ca^{2+} exchange by KB-R7943: transport mode selectivity and antiarrhythmic consequences. *Am J Physiol* **281:**H1334–H1345.

Haworth RA, Goknur AB, Hunter DR, Hegge JO, and Berkoff HA (1987) Inhibition of calcium influx in isolated adult rat heart cells by ATP depletion. *Circ Res* **60:**586–594.

Hilgemann DW (1997) Cytoplasmic ATP-dependent regulation of ion transporters and channels: mechanisms and messengers. *Annu Rev Physiol* **59:**193–220.

Hilgemann DW, Collins A, and Matsuoka S (1992a) Steady-state and dynamic properties of cardiac sodium-calcium exchange. Secondary modulation by cytoplasmic calcium and ATP. *J Gen Physiol* **100:**933–961.

Hilgemann DW, Matsuoka S, Nagel GA, and Collins A (1992b) Steady-state and dynamic properties of cardiac sodium-calcium exchange. Sodium-dependent inactivation. *J Gen Physiol* **100:**905–932.

Hotta Y, Lu X, Yajima M, Ishikawa N, Ito K, Inoue Y, and Sakaue T (2002) Protective effect of SN-6, a selective Na^+-Ca^{2+} exchange inhibitor, on ischemia-reperfusion-injured hearts. *Jpn J Pharmacol* **88**(Suppl)**:**257P.

Iwamoto T, Kita S, and Shigekawa M (2002) Functional analysis of Na^+/Ca^{2+} exchanger using novel drugs and genetically engineered mice. *Folia Pharmacol Jpn* **120:**91P–93P.

Iwamoto T, Kita S, Uehara A, Imanaga I, Matsuda T, Baba A, and Katsuragi T (2004) Molecular determinants of Na^+/Ca^{2+} exchange (NCX1) inhibition by SEA0400. *J Biol Chem* **279:**7544–7553.

Iwamoto T, Kita S, Uehara A, Inoue Y, Taniguchi Y, Imanaga I, and Shigekawa M (2001) Structural domains influencing sensitivity to isothiourea derivative inhibitor KB-R7943 in cardiac Na^+/Ca^{2+} exchanger. *Mol Pharmacol* **59:**524–531.

Iwamoto T, Nakamura TY, Pan Y, Uehara A, Imanaga I, and Shigekawa M (1999a) Unique topology of the internal repeats in the cardiac Na^+/Ca^{2+} exchanger. *FEBS Lett* **446:**264–268.

Iwamoto T, Pan Y, Nakamura TY, Wakabayashi S, and Shigekawa M (1998) Protein kinase C-dependent regulation of Na^+/Ca^{2+} exchanger isoforms NCX1 and NCX3 does not require their direct phosphorylation. *Biochemistry* **37:**17230–17238.

Iwamoto T, Uehara A, Imanaga I, and Shigekawa M (2000) The Na^+/Ca^{2+} exchanger NCX1 has oppositely oriented reentrant loop domains that contain conserved aspartic acids whose mutation alters its apparent Ca^{2+} affinity. *J Biol Chem* **275:**38571–38580.

Iwamoto T, Uehara A, Nakamura TY, Imanaga I, and Shigekawa M (1999b) Chimeric analysis of Na^+/Ca^{2+} exchangers NCX1 and NCX3 reveals structural domains important for differential sensitivity to external Ni^{2+} or Li^+. *J Biol Chem* **274:**23094–23102.

Iwamoto T, Watano T, and Shigekawa T (1996) A novel isothiourea derivative selectively inhibits the reverse mode of Na^+/Ca^{2+} exchange in cells expressing NCX1. *J Biol Chem* **271:**22391–22397.

Levitsky DO, Nicoll DA, and Philipson KD (1994) Identification of the high affinity Ca^{2+}-binding domain of the cardiac Na^+-Ca^{2+} exchanger. *J Biol Chem* **269:**22847–22852.

Li Z, Nicoll DA, Collins A, Hilgemann DW, Filoteo AG, Penniston JT, Weiss JN, Tomich JM, and Philipson KD (1991) Identification of a peptide inhibitor of the cardiac sarcolemmal Na^+-Ca^{2+} exchanger. *J Biol Chem* **266:**1014–1020.

Luthin GR and Wolfe BB (1984) Comparison of [^{3}H]pirenzepine and [^{3}H]quinuclidinylbenzilate binding to muscarinic cholinergic receptors in rat brain. *J Pharmacol Exp Ther* **228:**648–655.

Matsuda T, Arakawa N, Takuma K, Kishida Y, Kawasaki Y, Sakaue M, Takahashi K, Takahashi T, Suzuki T, Ota T, et al. (2001) SEA0400, a novel and selective inhibitor of the Na^+-Ca^{2+} exchanger, attenuates reperfusion injury in the in vitro and in vivo cerebral ischemic models. *J Pharmacol Exp Ther* **298:**249–256.

Matsuoka S, Nicoll DA, He Z, and Philipson KD (1997) Regulation of cardiac Na^+-Ca^{2+} exchanger by the endogenous XIP region. *J Gen Physiol* **109:**273–286.

Matsuoka S, Nicoll DA, Hryshko LV, Levitsky DO, Weiss JN, and Philipson KD (1995) Regulation of the cardiac Na^+-Ca^{2+} exchanger by Ca^{2+}. Mutational analysis of the Ca^{2+}-binding domain. *J Gen Physiol* **105:**403–420.

Nakamura A, Harada K, Sugimoto H, Nakajima F, and Nishimura N (1998) Effects of KB-R7943, a novel Na^+/Ca^{2+} exchange inhibitor, on myocardial ischemia/reperfusion injury. *Folia Pharmacol Jpn* **111:**105–115.

Nicoll DA, Hryshko LV, Matsuoka S, Frank JS, and Philipson KD (1996) Mutation of amino acid residues in the putative transmembrane segments of the cardiac sarcolemmal Na^+-Ca^{2+} exchanger. *J Biol Chem* **271:**13385–13391.

Nicoll DA, Ottolia M, Lu L, Lu Y, and Philipson KD (1999) A new topological model of the cardiac sarcolemmal Na^+-Ca^{2+} exchanger. *J Biol Chem* **274:**910–917.

Ogata M, Iwamoto T, Tazawa N, Nishikawa M, Takaoka M, Yamashita J, and Matsumura Y (2003) A novel and selective Na^+/Ca^{2+} exchange inhibitor, SEA0400, improves ischemia/reperfusion-induced renal injury. *Eur J Pharmacol* **478:**187–198.

Philipson KD and Nicoll DA (2000) Sodium-calcium exchange: a molecular perspective. *Annu Rev Physiol* **62:**111–133.

Pintado AJ, Herrero CJ, Garcia AG, and Montiel C (2000) The novel Na^+/Ca^{2+} exchange inhibitor KB-R7943 also blocks native and expressed neuronal nicotinic receptors. *Br J Pharmacol* **130:**1893–1902.

Qiu Z, Nicoll DA, and Philipson KD (2001) Helix packing of functionally important regions of the cardiac Na^+-Ca^{2+} exchanger. *J Biol Chem* **276:**194–199.

Quednau BD, Nicoll D, and Philipson KD (1997) Tissue specificity and alternative splicing of the Na^+/Ca^{2+} exchanger isoforms NCX1, NCX2 and NCX3 in rat. *Am J Physiol* **272:**C1250–C1261.

Reuter H, Henderson SA, Han T, Matsuda T, Baba A, Ross RS, Goldhaber JI, and Philipson KD (2002) Knockout mice for pharmacological screening: testing the specificity of Na^+-Ca^{2+} exchange inhibitors. *Circ Res* **91:**90–92.

Shigekawa M and Iwamoto T (2001) Cardiac Na^+-Ca^{2+} exchange: molecular and pharmacological aspects. *Circ Res* **88:**864–876.

Sobolevsky AI and Khodorov BI (1999) Blockade of NMDA channels in acutely isolated rat hippocampal neurons by the Na^+/Ca^{2+} exchange inhibitor KB-R7943. *Neuropharmacology* **38:**1235–1242.

Takahashi K, Takahashi T, Suzuki T, Onishi M, Tanaka Y, Hamano-Takahashi A, Ota T, Kameo K, Matsuda T, and Baba A (2003) Protective effects of SEA0400, a novel and selective inhibitor of the Na^+/Ca^{2+} exchanger, on myocardial ischemia-reperfusion injuries. *Eur J Pharmacol* **458:**155–162.

Tani M (1990) Mechanisms of Ca^{2+} overload in reperfused ischemic myocardium. *Annu Rev Physiol* **52:**543–559.

Watano T, Kimura J, Morita T, and Nakanishi H (1996) A novel antagonist, No. 7943, of the Na^+/Ca^{2+} exchange current in guinea-pig cardiac ventricular cells. *Br J Pharmacol* **119:**555–563.

Yamashita J, Kita S, Iwamoto T, Ogata M, Takaoka M, Tazawa N, Nishikawa M, Wakimoto K, Shigekawa M, Komuro I, et al. (2003) Attenuation of ischemia/reperfusion-induced renal injury in mice deficient in Na^+/Ca^{2+} exchanger. *J Pharmacol Exp Ther* **304:**284–293.

Address correspondence to: Dr. Takahiro Iwamoto, Department of Pharmacology, School of Medicine, Fukuoka University, 7-45-1 Nanakuma Jonan-ku, Fukuoka 814-0180, Japan. E-mail: tiwamoto@cis.fukuoka-u.ac.jp